engineering proceedings

MDPI

Proceeding Paper

VIV-Based Energy Harvesting from Tandem Cylinders for Self-Sustained IoT Systems †

Muhammad Mahad Shah, Usman Latif, Emad Uddin * and Syed Maaz Hasan

Department of Mechanical Engineering, School of Mechanical and Manufacturing Engineering, National University of Sciences and Technology, Islamabad 44000, Pakistan; muhammadmahad.pg@smme.edu.pk (M.M.S.); usmanlatif.phd16@smme.nust.edu.pk (U.L.); maaz.hasan@smme.nust.edu.pk (S.M.H.)

* Correspondence: emaduddin@smme.nust.edu.pk

† Presented at the 4th International Conference on Advances in Mechanical Engineering (ICAME-24), Islamabad, Pakistan, 8 August 2024.

Abstract: Piezoelectric energy harvesters are considered a replacement for batteries because they are self-sustainable with low or no maintenance, and suitable for off-grid devices. In this study, two cylinders were placed in a flowing stream of water. The upstream cylinder of 25 mm diameter is fixed at the center of the stream while another cylinder of the same diameter, which is free to oscillate in the crosswise direction of the flow and is placed in the wake of that fixed cylinder. A piezoelectric flag is then placed in the wake of the vibrating cylinder and its distance from the vibrating cylinder was changed to observe the effect of wake length on the energy harvester. The energy harvesting potential of the system is explored for flow velocities ranging from 0.28 m/s to 0.36 m/s. The distance between the cylinders Gx, which is explored for the range of 2.5D–7D, and the distance between the piezoelectric membrane and the vibrating cylinder are expressed as Sx for the same range. The maximum power of 19.17 μW was produced at Sx = 2D and Gx = 3.5D. The maximum power for the baseline case, when two tandemly arranged stationary circular cylinders were used and a piezoelectric membrane was placed in their wake, is 10.24 μW; hence, an increase of 87.2% is observed under the same ambient conditions.

Keywords: renewable energy; vortex-induced vibrations; energy harvesting; blockage ratio

Citation: Shah, M.M.; Latif, U.; Uddin, E.; Hasan, S.M. VIV-Based Energy Harvesting from Tandem Cylinders for Self-Sustained IoT Systems. *Eng. Proc.* **2024**, *75*, 40. https://doi.org/10.3390/engproc2024075040

Academic Editors: Muhammad Mahabat Khan, Muhammad Irfan, Mohammad Javed Hyder and Manzar Masud

Published: 8 October 2024

1. Introduction

Energy harvesting is an innovative method for supplying power to low-power wireless devices and sensors. It provides an eco-friendly alternative to conventional battery packs [1]. This technology utilizes ambient energy sources, such as mechanical vibrations, temperature gradients, and solar radiation, to produce electrical power. The harvesting systems have improved in tandem with the progress made in materials science, namely in the field of nanostructured materials and piezoelectric devices. Research to support the expanding number of Internet of Things (IoT) devices and remote sensors using energy-harvesting processes is ongoing [2].

Flow-induced vibration (FIV), a phenomenon generally considered hazardous for structural safety, can also be controlled [3] and utilized for energy harvesting [4]. There are in principle two types of FIVs: galloping and vortex-induced vibration (VIV) [5]. Galloping (a high-amplitude and low-frequency vibration) occurs when instabilities bring about oscillations at different amplitudes [6]. VIV, on the other hand, is a vibration caused by vortex shedding. Energy harvesting from VIVs is now an attractive avenue for researchers and has been enriched by the development of a significant number of energy-harvesting devices [7].

The inspiration to use VIVs for energy generation comes from aquatic organisms' utilization of vortex-induced propulsion mechanisms. The work of Smit and Allen [8]

is considered a benchmark of the field. They obtained electrical energy from the elastic motion of the membranes, leading to the exploration of VIVs for energy extraction. The model they used was an imitation of an eel that propels itself by undulating its body from side to side. Taylor et al. [9] applied this for energy extraction from natural aquatic resources. Various configurations have been developed to extract energy from spiral vibrations in fluid environments after that. Akaydin et al. [10] further improved this work by using piezoelectric beams of a smaller length downstream of a circular cylinder. They deduced that a distance of '2 diameters downstream' is the optimal placement for maximum power output. It decays as the distance-to-diameter ratio (x/D)-3/2 is increased further. Gao et al. [11] developed a novel device using a cantilever with piezoelectric materials attached to the cylinder. They tested the prototypes in both lower and higher Reynolds number flows. The consensus was that excitation occurring from turbulent flows provides significant improvement in power output. A similar work was conducted by Song et al. [12] with a vortex-induced piezoelectric energy harvester. Power of 84.49 μW was achieved with an energy density of 60.35 mW/m^2 at a 0.35 m/s resonance velocity. Instead of the more common circular cylinder, research has also been conducted in the past on square cylinders (among other shapes). Wang et al. [13] used a square cylinder attached to a spring vibrating freely in wind energy. Binyet et al. [14] studied the dimensional effects of a square cylinder and an attached plate. Shen and Wang [15] used a triangular-shaped body for their experiments in a flume environment with low-speed water. They showed that in galloping oscillations, the triangular bluff body performance is enhanced. A more comprehensive comparison of different cross-sections/shapes of bluff bodies was made by Wang et al. [16]. He concluded that for higher-voltage production, the spindle/circular-shaped bluff body is suitable provided it has a low width ratio.

For the scenario of multimodal shapes, Chen et al. [17] diverted from mono designs to a 'tri-directional' M-shaped harvester. Because of the unique shape, they utilized both bending and torsional energy harvesting modes. The combined bending torsion was also utilized by Li et al. [18] with an L-shaped structure for multi-directional, multi-mode harvesting. The L-shape has also been studied by Cao et al. [19] with a complete vibrational analysis. Additional multimodal shapes found in the literature include E-shaped [20], Bird-shaped [21], and fin-shaped attachments [22], among others.

Apart from the shape, bluff bodies in tandem arrangements with space considerations have also been explored in the literature. In the previous work of a co-author, Latif et al. [23] used a flexible piezoelectric eel at different wave conditions. A cylindrical bluff body was used with incremental changes in distance from the eel. They concluded that at a distance-to-diameter ratio of 1.25 produces the most favorable results. Latif et al. [24] also studied the effects of two cylinders on energy harvesting with a piezoelectric flag. In the research, cylinders were placed side by side and their gap with varying flow velocity was studied. It was concluded that four times higher amplitude and power can be achieved at the suitable positions. Mujtaba et al. [25] instead of multiple bluff bodies, researched multi-flag orientations with downstream configurations. Taking the work further, Ahmed et al. [26] worked on tandem-arranged cylinders with a flag as the piezoelectric material. After that, Mazharmanesh et al. [27] conducted extensive research on the energy extraction performance, as well as the flow-induced vibration, of two flexible inverted piezoelectric flags with tandem and side-by-side arrangements, among others. An important conclusion of this work was that the dynamics of the side-by-side configuration are independent of the cross-stream gap. Shah et al. [28] used a pivoted flapping mechanism in the wake of tandem cylinders. This provided a flapping amplitude gain of 51% and a frequency rise of 23%. Despite these investigations, limited research has been conducted on the specific effects of multiple bodies.

The literature reveals several existing tandem arrangements, yet there are numerous others that warrant exploration. In addition, a significant lack of experimental results can be seen. While there are some published simulation works on this topic, they have not been adequately validated through experimentation. In order to address this, the

present study focuses on utilizing VIV in low-speed channels or the ocean bed. This study utilizes a motionless circular cylinder as a stationary bluff body. Another circular cylinder is positioned downstream of the stationary cylinder, and it is capable of oscillating freely in the y-direction but constrained in the x-direction. A piezoelectric membrane is placed downstream of the vibrating cylinder to capture the vortex energy generated by both cylinders. The distance between the two bluff bodies (Gx) varied along with the distance of the membrane from the bluff bodies (Sx) to investigate the power-harvesting efficiency of the setup.

2. Methodology

The experimental setup utilized is in the Department of Mechanical Engineering of NUST in Islamabad, Pakistan [28]. The dimensions of the water channel test portion are 2000 by 400 by 400 mm (L × W × H). Using a variable frequency drive (VFD) motor, the free-stream velocity (U) can be changed from 0 to 0.5 m/s. Aluminum honeycombs with dimensions of 1830 mm by 500 mm by 25.4 mm are used to keep the flow rate constant. The bluff body used for this experiment consists of two circular aluminum cylinders. Each cylinder is 440 mm in length and 25 mm in diameter, with a wall thickness of 1.5 mm. Upstream cylinder was kept stationary, moving the second cylinder with the aid of VIVs, as presented in Figure 1.

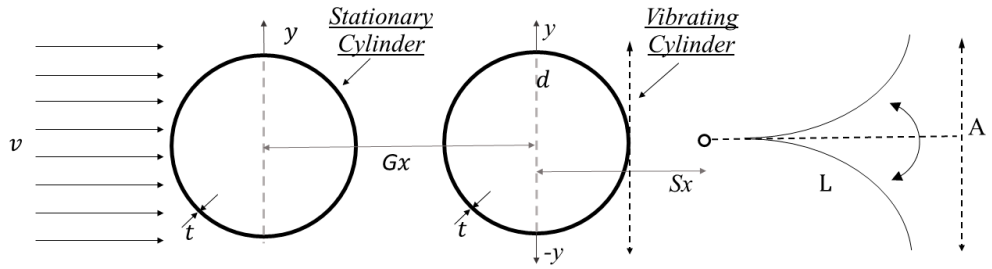

Figure 1. The figure depicts a flow (v) passing over the submerged cylinder. Gx = distance between the two cylinders in mm/diameter of the cylinder and Sx = distance between the vibrating cylinder and the piezoelectric eel in mm/diameter of the cylinder.

In the downstream of the vibrating cylinder, a piezoelectric membrane (manufacturer part number: 1-1002908-0, digikey part number: 223-1225-ND) is placed in the form of a flag. The leading edge of the flag is attached with a rod of 4 mm diameter, while the other end can move freely. The overall length of the membrane is 72 mm, although only 62 mm of it is usable due to its attachment with a 4 mm rod, and the piezo membrane is 64 mm in width (or 6.4 in). The intensity of the vibrations was measured with the help of a high-speed camera (Sony RX-100 IV) which grabs 1920 × 1080, 50 frames-per-second videos. MATLAB® 2022 and 2024 were used to analyze the video data and calculate the amplitude and flapping frequency of vibrations. The data are sampled at 50 Hz for 120 s from a data acquisition device or card (DAQ, NI-USB type 6009, multifunctional I/O) using LabView. The effect of varying velocity, the distance between the cylinders, and the distance between the vibratory cylinder and the piezoelectric flag was studied and strived to obtain more suitable quantities for these parameters.

3. Results and Discussion

This work used a multi-cylinder arrangement with a piezoelectric eel behind the downstream cylinder utilizing the VIVs. The list of experiments conducted with the variable flow speeds is presented in Table 1. Experiments were conducted, focusing on three key parameters: variable flow speed, the variable distance between cylinders (Gx), and the variable distance between the vibrating downstream cylinder and the power harvesting eel (Sx).

Table 1. List of experimental cases.

Variable G_x in terms of D	Variable flow speed "U" in m/s	Total Cases
2.5, 3, 3.5, 4, 4.5, 5, 5.5, 6, 6.5, and 7	0.28, 0.30, 0.32, 0.34 and 0.36	=50
Variable S_x in terms of D	**Variable flow speed "U" in m/s**	**Total Cases**
2.5, 3, 3.5, 4, 4.5, 5, 5.5, 6, 6.5, and 7	0.28, 0.30, 0.32, 0.34 and 0.36	=50
Total overall cases		=100

The stream-wise gap between the cylinders was systematically increased from 2.5D to 7D, with an increment of 0.5D to study flow dynamics. Furthermore, the velocity of the flow was deliberately varied within the range of 0.28 m/s to 0.36 m/s [23], enabling a detailed assessment of its impact on power generation. Additionally, the distance between the vibrating cylinder and the eel was incrementally extended from 2.5D to 7D, facilitating a thorough exploration of its influence on energy harvesting efficiency.

3.1. Effect of Gx

Power generation was computed across five discrete flow velocities, encompassing various streamwise gap configurations between the cylinders (Figure 2). The eel remained positioned at a constant distance of Sx = 2.5D from the vibratory cylinder throughout the experiments. Analysis revealed a noteworthy peak in power output at a flow velocity of 0.34 m/s. Notably, a consistent trend emerged, wherein escalating flow velocities correlated with enhanced power generation by the eel. This phenomenon is attributed to the amplification of vibration amplitude and piezoelectric eel frequency with increasing flow velocity, until reaching a critical threshold known as vortex-induced resonance. At this juncture, maximum power output, denoted as P_{max} and quantified at 18.45 μW, was attained, as depicted by the contours. Beyond this resonance point, no further amplification in power output was observed.

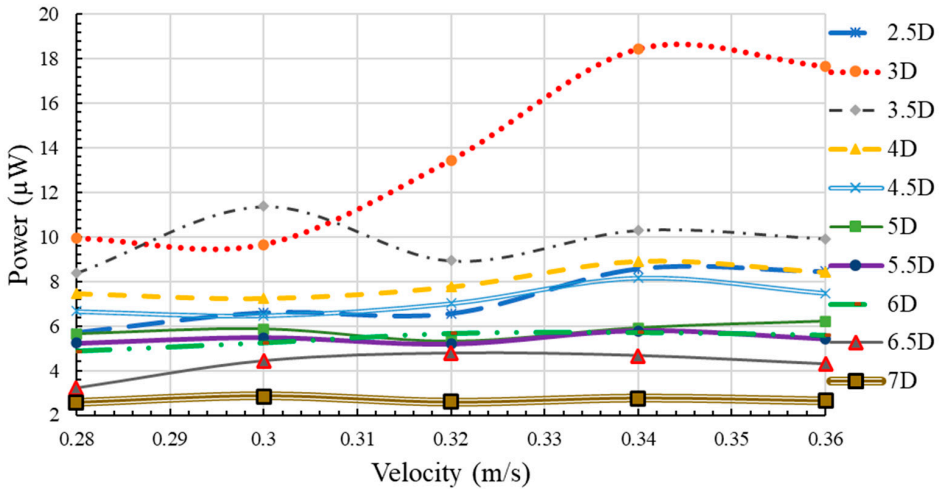

Figure 2. Power at different flow speeds for G_x values of 2.5–7D.

Moreover, an analogous trend was observed in graphical representations, although with a discernible decrease in power generation beyond 4D. It was observed that the apex power output was consistently obtained at 0.34 m/s and Gx = 3D across all cases (Figure 3). It was observed that beyond the optimal flow speed, there was negligible improvement in power generation. The influence of varying cylinder distances on fluid vortex interaction with the piezoelectric eel was examined, revealing an augmentation in power magnitude until 3D, beyond which a diminishing return was observed. Similarly, escalating flow velocities yielded higher power magnitudes until the vibratory eel frequency equaled the natural frequency, after which power generation plateaued.

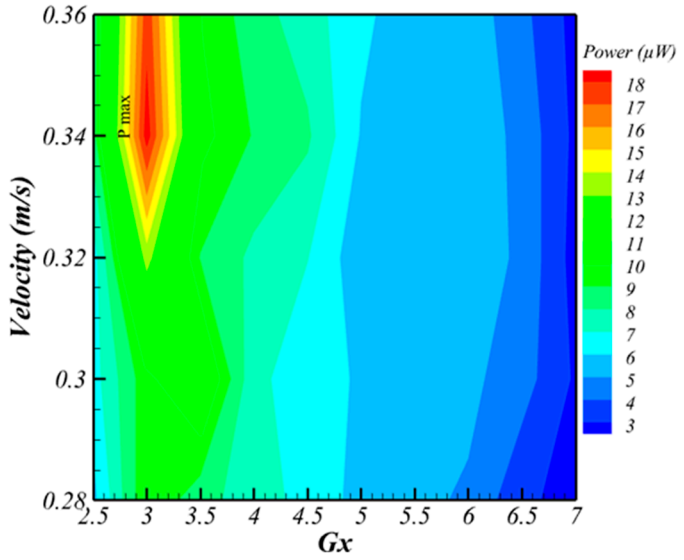

Figure 3. Power Contour for Gx Range of 2.5D to 7D.

To corroborate our findings, video footage was recorded at minimum velocity (v = 0.28 m/s) and peak power velocity, followed by analysis in MATLAB to ascertain eel oscillation amplitude ratio and frequency. This method of calculation is made possible by the work conducted by Latif et al. [24]. Figure 4 represents the flapping envelope, and the normalized frequency at Gx = 3D calculated through recorded video for 0.28 m/s is presented in Figure 4a, while the same for the velocity of 0.34 m/s is depicted in Figure 4b. The outcomes unequivocally affirm that the maximum A/L ratio and frequency were attained at Gx of 3D for both velocities, thereby validating our results. The A/L values exhibited an upward trajectory with increasing flow speed, corresponding to peak power generation. Similarly, analysis of eel frequency revealed that closer proximity of bluff bodies facilitated stronger vortex–eel interaction, resulting in higher frequency values. Conversely, a substantial increase in Gx weakened this interaction, precipitating a decline in eel frequency.

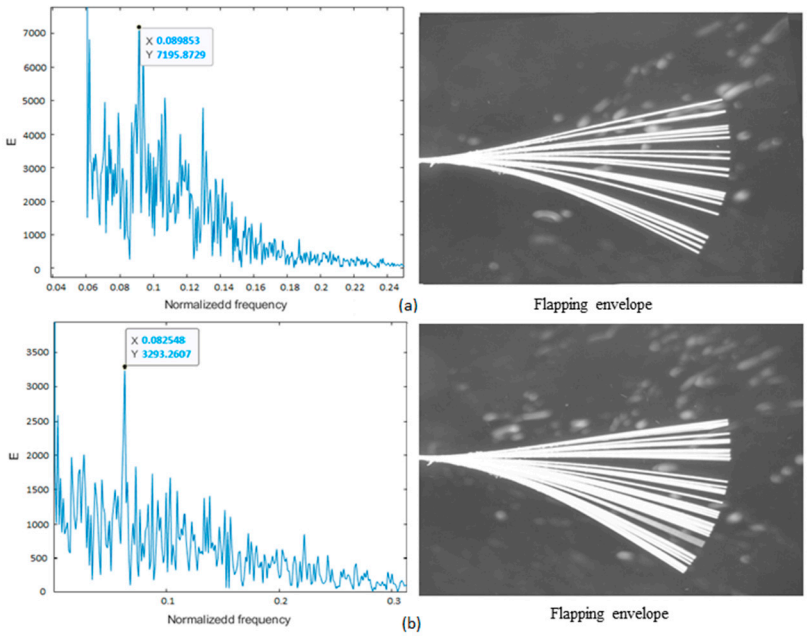

Figure 4. Normalized frequency and flapping of eel at (**a**) v = 0.28 m/s and (**b**) v = 0.34 m/s.

3.2. Effect of Changes in Sx

In the third series of experiments, the investigation focused on varying the streamwise distance from the vibratory cylinder to the piezoelectric flag. The objective was to ascertain the optimal placement of the piezoelectric flag to maximize power generation. The parameters used in the previous section were also upheld for the current set of experiments. The graphical representation of the experimental data in Figure 5 illustrates the power values obtained at various streamwise distances (S_x), with the maximum power occurring at S_x = 3.5D.

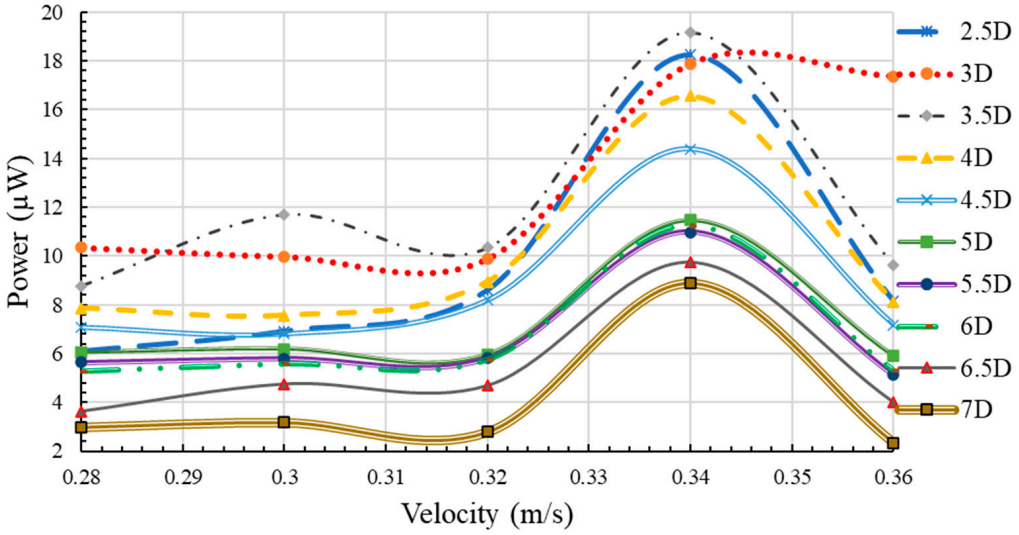

Figure 5. Power at different flow speeds for S_x values of 2.5–7D.

The power harvested at 3D is also higher compared to other distances, but beyond 4D, a decline in power is observed. This may be attributed to the loss of vortex turbulent energy beyond this distance due to the vibration-damping property of water. As anticipated, the lowest power magnitude was recorded at S_x = 7D, attributed to the diminished vibration amplitude in both the cylinder and the piezoelectric flag at this distance. Furthermore, Figure 6 depicts the contour plots of power and A/L values obtained, with P_{max} representing the peak power output.

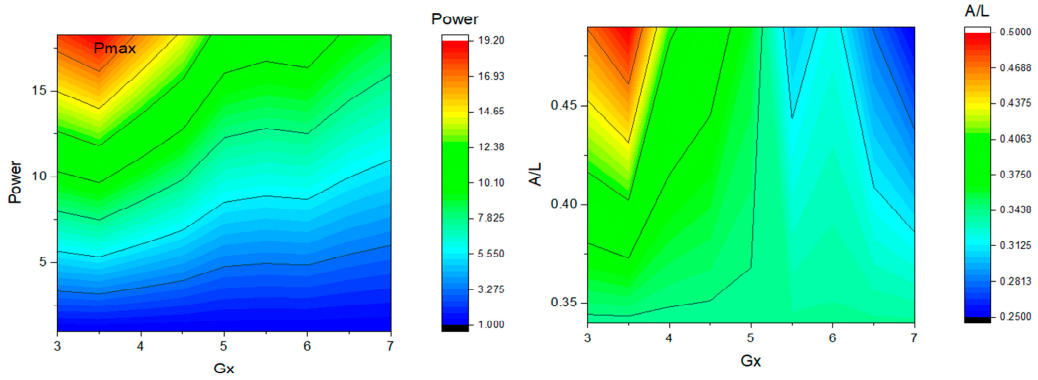

Figure 6. Power and A/L contour for S_x range of 2.5D to 7D.

To corroborate these findings, the vibration amplitude ratio and frequency of the eel were meticulously calculated using recorded video footage of the vibratory eel at different S_x values corresponding to the power harvesting experiments. Subsequent analysis of this footage yielded insightful results. The graphical representation of these findings is presented in Figure 7. The two stationary, tandemly arranged cylinders, each with a diameter of 25 mm, were used as blunt bodies. The same flag was used under identical ambient conditions to measure the energy output of the system. The harvested power

for the baseline case is reported to be 10.24 μW, as presented in Figure 7, providing an improvement of 87.2% over the baseline case. These results indicate the viability of this energy harvesting mechanism as a simplistic yet effective means of power generation.

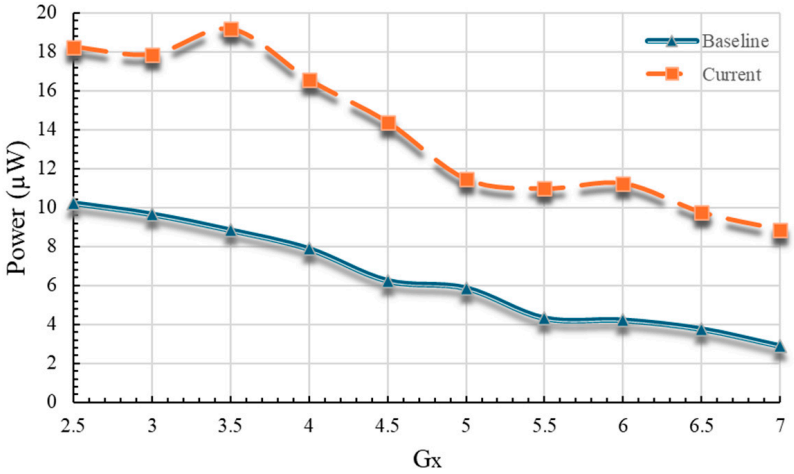

Figure 7. Power comparison with the baseline case at a flow velocity of 0.34 m/s.

4. Conclusions

In the current study, a series of experiments was conducted utilizing three distinct sets of parameters on two tandem-arranged cylinders, one of which was set in vibratory motion within the downstream flow. Our focus centered on analyzing the amplitude of vibration and the power harvested, resulting in several insightful findings. In the initial set of experiments, an augmentation in flow speed was observed, which was related to an increase in harvested power until the attainment of vortex-induced resonance at 0.34 m/s. Beyond this point, no further enhancement in power magnitude was detected. The second set of experiments involved the deliberate variation in the streamwise gap (G_x) between the two cylinders, ranging from 2.5D to 7D. While an overall increase in power magnitude was noted, the apex power output was achieved at 3D. Beyond this, a diminishing trend in power magnitude was observed. In the third set of experiments, we explored the impact of increasing the distance (S_x) between the vibratory cylinder and the piezoelectric flag, varying from 2.5D to 7D. Optimal power values were attained when the flag was positioned at 3.5D, with diminishing power observed beyond this point. A thorough verification process involved the calculation of A/L, frequency, and amplitude of the vibrating eel, validating our experimental results.

Author Contributions: Conceptualization, M.M.S. and E.U.; methodology, M.M.S. and E.U.; software, M.M.S.; validation, M.M.S., E.U., S.M.H. and U.L.; formal analysis, M.M.S. and E.U.; investigation, M.M.S.; resources, M.M.S. and E.U.; data curation, M.M.S. and S.M.H.; writing—original draft preparation, M.M.S. and S.M.H.; writing—review and editing, M.M.S., S.M.H. and U.L. All authors have read and agreed to the published version of the manuscript.

Funding: This research received no external funding.

Institutional Review Board Statement: Not applicable.

Informed Consent Statement: Not applicable.

Data Availability Statement: The raw data supporting the conclusions of this article will be made available by the authors on request.

Acknowledgments: We extend our heartfelt gratitude to our colleagues, fellow researchers, and research scholars at the School of Mechanical and Manufacturing Engineering, NUST, for their invaluable insights and expertise, which made this work possible. Their dedication and support have been instrumental in advancing our research. Moreover, we would like to pay our thanks to NUST H12, Islamabad, for allowing us to perform our experiments in the Flow visualization lab of SMME.

Conflicts of Interest: The authors declare no conflicts of interest.

References

1. Sezer, N.; Koç, M. A Comprehensive Review on the State-of-the-Art of Piezoelectric Energy Harvesting. *Nano Energy* **2021**, *80*, 105567. [CrossRef]
2. Sanislav, T.; Mois, G.D.; Zeadally, S.; Folea, S.C. Energy Harvesting Techniques for Internet of Things (IoT). *IEEE Access* **2021**, *9*, 39530–39549. [CrossRef]
3. Zhao, M. A Review of Recent Studies on the Control of Vortex-Induced Vibration of Circular Cylinders. *Ocean Eng.* **2023**, *285*, 115389. [CrossRef]
4. Ma, X.; Zhou, S. A Review of Flow-Induced Vibration Energy Harvesters. *Energy Convers. Manag.* **2022**, *254*, 115223. [CrossRef]
5. Rabiee, A.H. Galloping and VIV Control of Square-Section Cylinder Utilizing Direct Opposing Smart Control Force. *J. Theor. Appl. Vib. Acoust.* **2019**, *5*, 69–84. [CrossRef]
6. Mannini, C.; Marra, A.M.; Bartoli, G. VIV–Galloping Instability of Rectangular Cylinders: Review and New Experiments. *J. Wind Eng. Ind. Aerodyn.* **2014**, *132*, 109–124. [CrossRef]
7. Wang, J.; Geng, L.; Ding, L.; Zhu, H.; Yurchenko, D. The State-of-the-Art Review on Energy Harvesting from Flow-Induced Vibrations. *Appl. Energy* **2020**, *267*, 114902. [CrossRef]
8. Allen, J.J.; Smits, A.J. Energy Harvesting Eel. *J. Fluids Struct.* **2001**, *15*, 629–640. [CrossRef]
9. Taylor, G.W.; Burns, J.R.; Kammann, S.A.; Powers, W.B.; Welsh, T.R. The Energy Harvesting Eel: A Small Subsurface Ocean/River Power Generator. *IEEE J. Ocean. Eng.* **2001**, *26*, 539–547. [CrossRef]
10. Akaydın, H.D.; Elvin, N.; Andreopoulos, Y. Wake of a Cylinder: A Paradigm for Energy Harvesting with Piezoelectric Materials. *Exp. Fluids* **2010**, *49*, 291–304. [CrossRef]
11. Gao, X.; Shih, W.-H.; Shih, W.Y. Flow Energy Harvesting Using Piezoelectric Cantilevers With Cylindrical Extension. *IEEE Trans. Ind. Electron.* **2013**, *60*, 1116–1118. [CrossRef]
12. Song, R.; Shan, X.; Lv, F.; Xie, T. A Study of Vortex-Induced Energy Harvesting from Water Using PZT Piezoelectric Cantilever with Cylindrical Extension. *Ceram. Int.* **2015**, *41*, S768–S773. [CrossRef]
13. Wang, J.; Wen, S.; Zhao, X.; Zhang, M.; Ran, J. Piezoelectric Wind Energy Harvesting from Self-Excited Vibration of Square Cylinder. *J. Sens.* **2016**, *2016*, 1–12. [CrossRef]
14. Binyet, E.M.; Chang, J.-Y.; Huang, C.-Y. Flexible Plate in the Wake of a Square Cylinder for Piezoelectric Energy Harvesting—Parametric Study Using Fluid–Structure Interaction Modeling. *Energies* **2020**, *13*, 2645. [CrossRef]
15. Shen, Y.; Wang, J. Energy Harvesting by Applying VIV with a Circular Cylinder and Galloping with a Triangle Cylinder in a Low-Speed Water Flume. In Proceedings of the 32nd International Ocean and Polar Engineering Conference, Shanghai, China, 5 June 2022; p. ISOPE-I-22-079.
16. Wang, J.; Zhang, C.; Gu, S.; Yang, K.; Li, H.; Lai, Y.; Yurchenko, D. Enhancement of Low-Speed Piezoelectric Wind Energy Harvesting by Bluff Body Shapes: Spindle-like and Butterfly-like Cross-Sections. *Aerosp. Sci. Technol.* **2020**, *103*, 105898. [CrossRef]
17. Chen, K.; Gao, F.; Liu, Z.; Liao, W.-H. A Nonlinear M-Shaped Tri-Directional Piezoelectric Energy Harvester. *Smart Mater. Struct.* **2021**, *30*, 045017. [CrossRef]
18. Li, H.; Liu, D.; Wang, J.; Shang, X.; Hajj, M.R. Broadband Bimorph Piezoelectric Energy Harvesting by Exploiting Bending-Torsion of L-Shaped Structure. *Energy Convers. Manag.* **2020**, *206*, 112503. [CrossRef]
19. Cao, Y.; Cao, D.; He, G.; Ge, X.; Hao, Y. Vibration Analysis and Distributed Piezoelectric Energy Harvester Design for the L-Shaped Beam. *Eur. J. Mech.–A Solids* **2021**, *87*, 104214. [CrossRef]
20. Xie, Z.; Liu, L.; Huang, W.; Shu, R.; Ge, S.; Xin, Y.; Chen, Z.; Lin, W. A Multimodal E-Shaped Piezoelectric Energy Harvester with a Built-in Bistability and Internal Resonance. *Energy Convers. Manag.* **2023**, *278*, 116717. [CrossRef]
21. Yu, H.; Zhang, X.; Shan, X.; Hu, L.; Zhang, X.; Hou, C.; Xie, T. A Novel Bird-Shape Broadband Piezoelectric Energy Harvester for Low Frequency Vibrations. *Micromachines* **2023**, *14*, 421. [CrossRef]
22. Song, T.; Ding, L.; Yang, L.; Ran, J.; Zhang, L. Comparison of Machine Learning Models for Performance Evaluation of Wind-Induced Vibration Piezoelectric Energy Harvester with Fin-Shaped Attachments. *Ocean Eng.* **2023**, *280*, 114630. [CrossRef]
23. Latif, U.; Ali, E.; Uddin, E.; Ali, Z.; Sajid, M.; Shah, S.R.; Younis, M.Y. Experimental Investigation of Energy Harvesting Eel in the Wake of Bluff Body under Ocean Waves. *Proc. Inst. Mech. Eng. Part M J. Eng. Marit. Environ.* **2021**, *235*, 81–92. [CrossRef]
24. Latif, U.; Younis, M.Y.; Idrees, S.; Uddin, E.; Abdelkefi, A.; Munir, A.; Zhao, M. Synergistic Analysis of Wake Effect of Two Cylinders on Energy Harvesting Characteristics of Piezoelectric Flag. *Renew. Sustain. Energy Rev.* **2023**, *173*, 113114. [CrossRef]
25. Mujtaba, A.; Latif, U.; Uddin, E.; Younis, M.Y.; Sajid, M.; Ali, Z.; Abdelkefi, A. Hydrodynamic Energy Harvesting Analysis of Two Piezoelectric Tandem Flags under Influence of Upstream Body's Wakes. *Appl. Energy* **2021**, *282*, 116173. [CrossRef]
26. Ahmed, A.; Kashif, M.; Rehman, U.U. Energy Harvesting in The Wake of Two Tandem Arranged Cylinders with Downstream Vibrating Cylinder. In Proceedings of the 13th Asian Computational Fluid Dynamics Conference (ACFD 2022), Jeju, Republic of Korea, 16–19 October 2022; pp. 306–307.

27. Mazharmanesh, S.; Young, J.; Tian, F.-B.; Ravi, S.; Lai, J.C.S. Coupling Performance of Two Tandem and Side-by-Side Inverted Piezoelectric Flags in an Oscillating Flow. *J. Fluids Struct.* **2023**, *119*, 103874. [CrossRef]
28. Shah, M.M.; Mahmood, R.; Latif, U.; Uddin, E.; Munir, A.; Zhao, M.; Riaz, H.H. Experimental Investigation of the Wake of Tandem Cylinders Using Pivoted Flapping Mechanism for Piezoelectric Flag. *Ocean Eng.* **2024**, *310*, 118587. [CrossRef]